Low Surface Energy Polymeric Films from Solventless Liquid Oligoesters and Partially Fluorinated Isocyanates

W. Ming,*,† M. Tian,‡ R. D. van de Grampel,† F. Melis,† X. Jia,§ J. Loos,‡ and R. van der Linde†

Laboratory of Coatings Technology and Dutch Polymer Institute, Eindhoven University of Technology, P.O. Box 513, 5600 MB Eindhoven, The Netherlands, and Polymer Science and Engineering Department, University of Massachusetts, Amherst, Massachusetts 01003

Received April 26, 2002; Revised Manuscript Received July 3, 2002

ABSTRACT: Partially fluorinated isocyanates were synthesized from hexamethylene diisocyanate (HDI) and an HDI trimer (Desmodur N3300). The perfluoroalkyl group (R_f) was C_6F_{13} or C_8F_{17}, and the ratio between R_f and the isocyanate group (NCO) was 1/99 in the case of HDI or 1/49 in the case of N3300. Polymeric films with surface energies as low as 10 mN/m were obtained from mixtures of these partially fluorinated isocyanates and a previously reported hydroxyl-end-capped solventless liquid oligoester. Contact angles of water and hexadecane reached 120° and 80°, respectively, when less than 1 wt % of fluorine was present in the films. The surface enrichment of fluorine-containing species was confirmed by X-ray photoelectron spectroscopy (XPS) investigations. At a fluorine concentration of 0.5−1.0 wt %, the surface F/C atomic ratio (at a 15° takeoff angle) was greater than 1; the surface enrichment factor of fluorine was up to 600. The topological structures of the polymeric films were recorded by an atomic force microscope under tapping mode. While the height images indicated that the surface was smooth at the nanometer scale in a 1 μm × 1 μm area, the phase images revealed that fluorine-enriched domains were present at the surface. As the fluorine concentration increased, the fluorine-enriched domains grew from tiny spots (2−3 nm) to larger round domains (15−25 nm in diameter). The low surface energies of the films could be ascribed to the strong surface segregation of fluorinated species.

Introduction

Fluorinated polymers have demonstrated many properties that are desirable in coatings, for example, excellent hydrophobicity and oleophobicity, low coefficients of friction, excellent chemical resistance, and good weatherability.[1−5] Conventional fluoropolymer coatings, e.g., poly(tetrafluoroethylene) (PTFE) and poly(vinylidene fluoride) (PVDF), besides their high cost, are generally difficult to process. Recently developed perfluoropolyethers (PFPEs)[6,7] and copolymers of fluoroethylene and alkyl vinyl ether (FEVE)[8,9] can be soluble in organic solvents and have shown some promising properties, but the synthesis and the high cost due to the high fluorine content remain a big challenge.

On the other hand, water/oil repellency (low friction coefficient as well) is basically a surface property, not a bulk property. It is, therefore, unnecessary to have the expensive fluorine in the bulk. The good water/oil repellency is especially due to the low surface energy of the fluorinated films, and there has been a considerable amount of interest to prepare fluorinated films.[10−26] Self-stratification[27−29] strategies may provide an excellent opportunity to create surface coatings, in which desired surface and bulk properties are well balanced. In such an approach, only a very small quantity of fluorinated species is needed to provide a surface with low surface energy. The fluorinated species would migrate toward the air/film interface to minimize the interfacial energy.[1,2,10,11,24,25]

We have recently developed low surface energy cross-linked films on the basis of partially fluorinated hydroxyl-end-capped solventless liquid oligoesters, either thermally cured[30] with a polyisocyanate or photocured[31] after the introduction of acrylic double bonds. The addition of 1−1.5 wt % of fluorine could reduce the surface energy by 15−25 mN/m.[30,31] The surface enrichment of fluorinated species was confirmed by X-ray photoelectron spectroscopy (XPS) investigations; the fluorine level in the outermost 5 nm depth was about 20−80-fold above its bulk level. The driving force for the surface segregation of fluorinate species came from the large difference in surface energy between the fluorinated species and nonfluorinated components.[4,17,21−23]

Surface segregation of fluorinated species during film formation is a matter of competition between the diffusion of fluorinated species and the formation of cross-linked network. The current work aims at improving the diffusivity of the fluorinated species toward even more pronounced surface enrichment of fluorinated species. Instead of the previously used partially fluorinated oligoesters,[30−32] linear and 3-armed polyisocyanates were partially fluorinated and subsequently mixed with non-fluorinated liquid oligoesters to produce low surface energy films. The cross-linking reaction between the isocyanate and hydroxyl groups was monitored by ATR (attenuated total reflectance) FTIR. The fluorine enrichment in the top surface of the films was examined by contact angle measurements and X-ray photoelectron spectroscopy (XPS). Topology of the low surface energy films was examined by tapping mode atomic force microscopy (AFM).

Experimental Section

Materials. Two different perfluoroalkyl alcohols, $C_nF_{2n+1}CH_2CH_2OH$ (n = 6 and 8, denoted as F6-OH and F8-OH,

† Laboratory of Coatings Technology, Eindhoven University of Technology.
‡ Dutch Polymer Institute, Eindhoven University of Technology.
§ University of Massachusetts.
* Corresponding author: Fax 31-40-2463966; e-mail W.Ming@tue.nl.

10.1021/ma020650i CCC: $22.00
Published on Web 07/30/2002

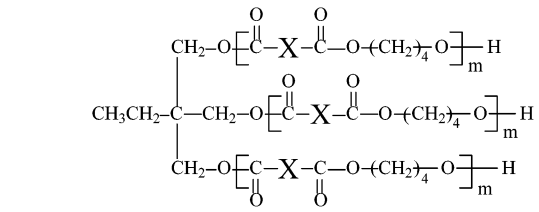

X = equimolar mixture of $(CH_2)_3$, $(CH_2)_4$, and $(CH_2)_7$; m = 1-2

(a)

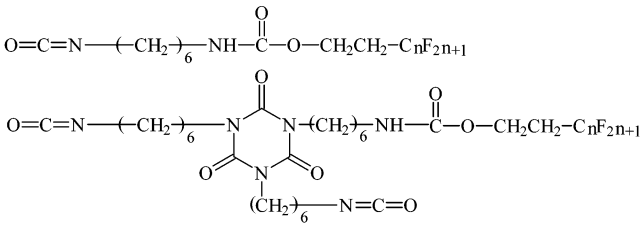

n = 6, 8

C_nF_{2n+1}/NCO = 1/49 (N3300) and 1/99 (HDI)

(b)

Figure 1. Chemical structures of (a) a 3-armed solventless liquid oligoester (SLO) and (b) partially fluorinated isocyanates.

respectively), were kindly supplied by Clariant GmbH (with trademarks of Fluowet EA 600 and EA 800, respectively). Hexamethylene diisocyanate (HDI) and a HDI trimer (Desmodur N3300) were obtained from Merck and Bayer AG, respectively. Other chemicals were purchased from Merck and used as received, unless otherwise stated. Aluminum panels ($0.6 \times 76 \times 152$ mm^3) were purchased from Q-Panel Co.

A Solventless Liquid Oligoester (SLO). The synthesis of a 3-armed solventless liquid oligoester (SLO) has been detailed elsewhere.[30,32] An ideal structure is shown in Figure 1, but the product is actually a mixture of different compositions. The number-average molecular weight for this oligoester was estimated to be 914 from ^{1}H NMR. The molar amount of hydroxyl groups in 1 g of the oligoester was 3.56×10^{-3} mol as determined by titration. The glass transition temperature of this oligoester was determined to be −60 °C on a Perkin-Elmer Pyris 1 differential scanning calorimeter at a heating rate of 10 °C/min, and no melting temperature was detected.

Synthesis of Partially Fluorinated Isocyanates. In general, the molar ratio between the perfluoroalkyl (R_f) group and NCO was controlled at either 1/99 (in the case of HDI) or 1/49 (in the case of N3300), as schematically shown in Figure 1. A typical reaction between HDI and F6-OH is described as follows. To a 250 mL three-neck flask equipped with a magnetic stirrer, an addition funnel, a reflux condenser, a thermocouple, and nitrogen inlet was added 42.0 g of HDI (0.25 mol) and 10 mg of dibutyltin dilaurate (a catalyst). After the flask was heated to 70 °C, 1.82 g of F6-OH (0.005 mol) was added dropwise through the addition funnel. The reaction was maintained at 70 °C for 2 h. The product (F6-HDI) was stored in a sealed container under argon atmosphere to avoid the contact with atmospheric moisture. Other fluorinated isocyanates, including F8-HDI, F6-N3300, and F8-N3300, were synthesized in a similar way except the reactions were performed in dried THF. THF was vacuum-distilled after reactions.

Film Preparation. A partially fluorinated isocyanate was mixed with an appropriate amount of the liquid oligoester under magnetic stirring. Nonfluorinated polyisocyanates (e.g., HDI and N3300) were also added in order to vary the fluorine concentration in the films. The overall OH/NCO molar ratio was maintained at about 1. After a homogeneous mixture was formed, a coating was drawn down on a clean aluminum panel with a square applicator. The coating was then cured at 80 °C for 1 h. The thickness for dry films was found to be about 20 μm, as measured using a Twin-Check thickness gauge by List-Magnetic GmbH.

Table 1. NCO Contents in Isocyantates and Partially Fluorinated Isocyanates

isocyanate	theor amount (wt %)	measd amount (wt %)
HDI	50.00	49.58
F6-HDI-I[a]	48.26[b]	45.08
F8-HDI	46.53[b]	45.16
N3300	21.54	20.13
F6-N3300	19.40[b]	19.56
F8-N3300	19.21[b]	19.22

[a] In F6-HDI-I, R_f/NCO = 1/199. [b] Measured NCO contents for HDI and N3300 were used for the calculation of these theoretical values.

Characterizations. ^{1}H and ^{19}F NMR spectra were recorded on a Varian 400 spectrometer at 25 °C with $CDCl_3$ as a solvent. Contact angles were measured with deionized water and hexadecane (>99%, Merck) on a contact angle microscope (G10, Krüss, Hamburg). Dynamic advancing angles were recorded while the probe liquid was added to the drop by a syringe pump. Static contact angles were also recorded. The contact angle reported is the average of values for 3−4 drops, and the difference was normally within 2°. Surface tension of liquid samples was measured by the Wilhelmy plate method on a Kruss digital tensiometer K10T. XPS spectra were collected on a Perkin-Elmer-Physical Electronics 5100 spectrometer with monochromatic Mg Kα excitation (400 W). Spectra were acquired at three different takeoff angles: 15°, 45°, and 75° (between the film plane and the entrance lens of the detector optics). All C_{1s} peaks corresponding to hydrogen carbon were calibrated at a binding energy of 285.0 eV to correct for charging.[15,30,31] Real-time infrared spectra were recorded on a BioRad Excalibur spectrophotometer equipped with a mercury−cadmium−telluride (MCT) detector, a MKII Golden Gate heated diamond 45° ATR top plate (Specac Ltd., Kent, England), and a 3000 series high stability temperature controller (Specac). After a reaction mixture was deposited on the diamond unit, infrared spectra (eight scans per spectrum) were collected every 20−30 s at a resolution of 4 cm^{-1}. Atomic force microscopy (AFM) images (both height and phase) were recorded simultaneously under tapping mode on a Dimension 3100 AFM (Digital Instruments, Santa Barbara, CA), operated in air. A noncontact "golden" silicon cantilevel, NSG01 (NT-MDT, Moscow, Russia), with a spring force constant of 11−15 N/m, was used. Typical resonance frequencies were in the range 210−230 kHz. The set point amplitude was adjusted for "light-force" tapping,[42,43] unless otherwise stated.

Results and Discussion

Synthesis of Partially Fluorinated Isocyanates. Partially fluorinated isocyanates were prepared by reacting isocyanates with perfluoroalkyl (R_f) alcohols. The molar ratio between R_f and NCO was controlled at 1/49 (in the case of HDI trimer) and 1/99 (in the case of HDI) to avoid the formation of all-perfluoroalkyl-substituted species, which, otherwise, would not be chemically bonded to the final cross-linked network. Proton NMR was used to monitor the partial fluorination. In the case of F6-HDI, after the partial fluorination the peak at 4.0 ppm (R_f−$CH_2C\boldsymbol{H}_2$−OH) of alcohol disappeared completely, and instead, a new peak emerged at 4.2−4.3 ppm (R_f−$CH_2C\boldsymbol{H}_2$−OCO−NH−), indicating that the perfluoroalkyl groups were completely bonded to the isocyanates. The monosubstituted species was clearly shown in the matrix-assisted laser desorption ionization time-of-flight (MALDI−TOF) mass spectrum, while no bisubstituted species was detected. In addition, the NCO content was checked by the titration method specified in ASTM D2572-91 before and after the partial fluorination. As shown in Table 1,

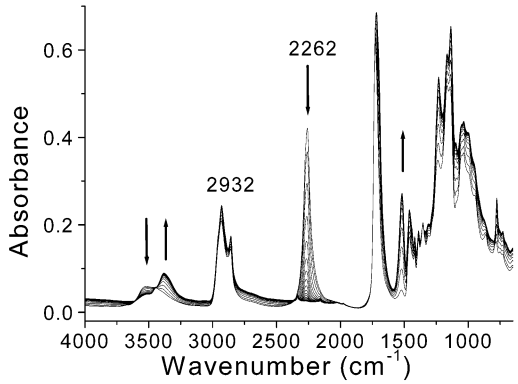

Figure 2. Real-time ATR−FTIR spectra for the thermal curing of SLO by HDI at 80 °C.

for the partially fluorinated isocyanates, the experimental values are only slightly different with the theoretical ones, indicating that there were almost no side reactions during the partial fluorination process.

Thermal Curing of SLO with Isocyanates. The reactions between hydroxyl-end-capped oligoesters and isocyanates were monitored by real-time ATR−FTIR. The evolution of IR spectra of the reaction mixture of HDI and the oligoester (SLO) at 80 °C is shown in Figure 2. The peak at 2262 cm^{-1}, corresponding to the NCO group, decreased steadily as the curing reaction proceeded; so did the peak at 3530 cm^{-1} (OH stretching). New peaks emerged at 3380 cm^{-1} (−NH−COO−, N−H stretching) and at 1520 cm^{-1} (−NH−COO−, N−H bending). On the other hand, the CH_2 stretch (2932 cm^{-1}) remained the same throughout the reaction, which can be taken as an internal standard for the study on the cross-linking. It can be seen that the hydroxyl absorbance did not disappear completely, indicating the hydroxyl group was in a little excess. But the attention will be paid mainly on the disappearance of the NCO peak.

The peak area ratio between 2262 and 2932 cm^{-1} is plotted as a function of reaction time for both HDI and N3300 in Figure 3. For the reaction between HDI and SLO at 80 °C, this ratio kept decreasing before reaching a minimum, as given in Figure 3a. Correspondingly, the conversion of NCO during the curing could be calculated, as also shown in Figure 3a. The complete consumption of the NCO group was reached in a period of about 7 min. The reaction between SLO and partially fluorinated HDI (F6-HDI) at 80 °C was also monitored; the existence of fluorine did not show any significant effect on the cross-linking. This is reasonable as far as the small amount of fluorine (about 1.4 wt %) in F6-HDI is concerned.

Real-time IR spectra were also collected for the reaction between N3300 and SLO. At 80 °C (Figure 3b), the reaction between N3300 and SLO, which reached the complete conversion of NCO in about 40 min, proceeded much slower than that between HDI and SLO. This is primarily due to the higher viscosity of the reaction mixture of N3300 and SLO; the mobility of both NCO and OH may decrease in comparison with that in the mixture of HDI and SLO. Therefore, the linear diisocyanate reacts much faster with hydroxyls in an oligoester than the 3-armed polyisocyanate.

The reaction temperature has also demonstrated a tremendous effect on the cross-linking between NCO and OH groups. In general, the lower the reaction temperature was, the *much* slower the cross-linking

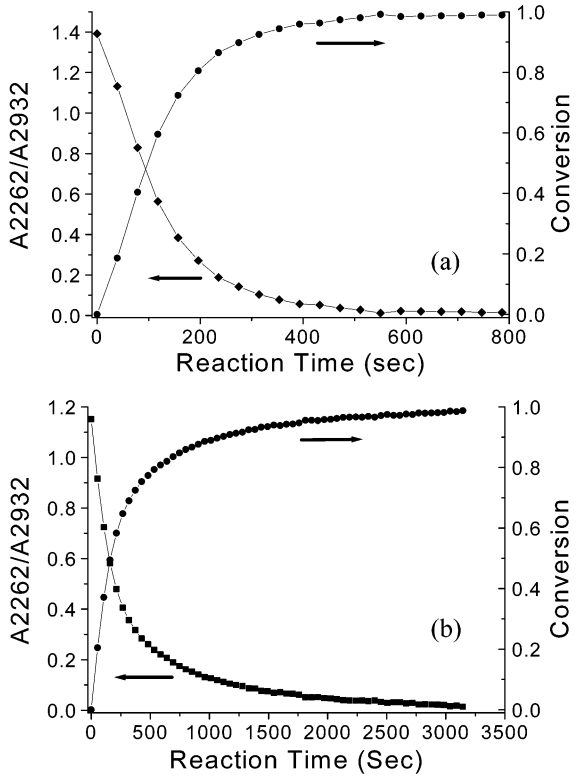

Figure 3. Conversion of NCO during thermal curing of SLO at 80 °C by (a) HDI and (b) N3300.

proceeded. For instance, for the reaction between HDI and SLO at 40 °C, it took more than 3 h for NCO conversion to reach 90%. This is a subject concerning the opposite effects of reaction temperature on the formation rate of cross-linked network and on the diffusion of fluorinated species and has been discussed in detail in another paper.[33]

Surface Properties of the Films from SLO and Partially Fluorinated Isocyanates. Contact angle of a liquid on a film surface is a direct reflection of the hydrophilicity/hydrophobicity of the surface.[34] In this study water and hexadecane were chosen as probe liquids. The surface tensions can be estimated by the geometric mean method[35] on the basis of contact angles of the two liquids.

Advancing contact angles of water and static contact angles of hexadecane on films based on fluorinated HDIs (F6-HDI and F8-HDI) and SLO, as a function of the added fluorine content in the films (calculated from the recipes by assuming complete conversions of all reactions; see Experimental Section), are shown in Figure 4. In the case of F6-HDI, the water contact angle kept increasing from about 82° to 120°, and the hexadecane contact angle showed a similar trend (from 0° to 60°), when the added fluorine content in the films increased up to about 0.7 wt %. (No further increase was possible, since the NCO/OH had to be kept at 1.) No plateau was observed for both curves. On the other hand, when F8-HDI was used, the increase of both water and hexadecane contact angles was much more pronounced upon the addition of a small amount of fluorinated species, also shown in Figure 4a,b; for the hexadecane angle, it reached 80°. The contact angles leveled off when the fluorine content was greater than 0.6 wt %. These high contact angles demonstrated clearly that the surface of the films was significantly enriched in the fluorinated species. The difference in the effect between F8-HDI and

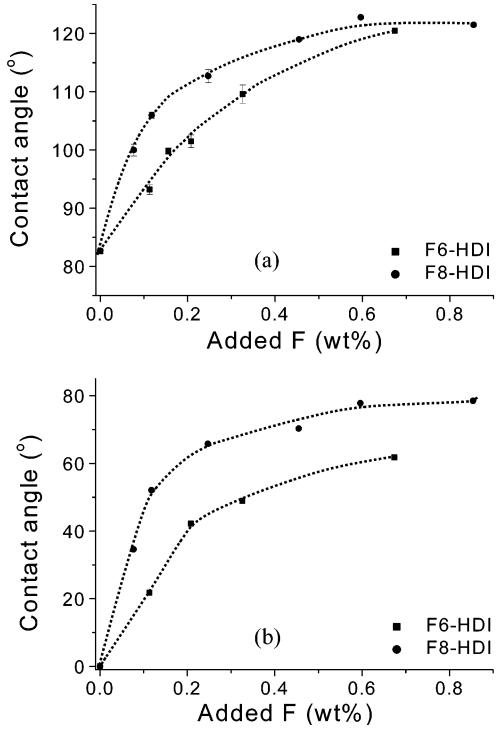

Figure 4. Advancing contact angles of water (a) and static contact angles of hexadecane (b) on polymer films, from SLO and partially fluorinated HDIs (F6-HDI and F8-HDI) cured at 80 °C, as a function of the added fluorine content in the films.

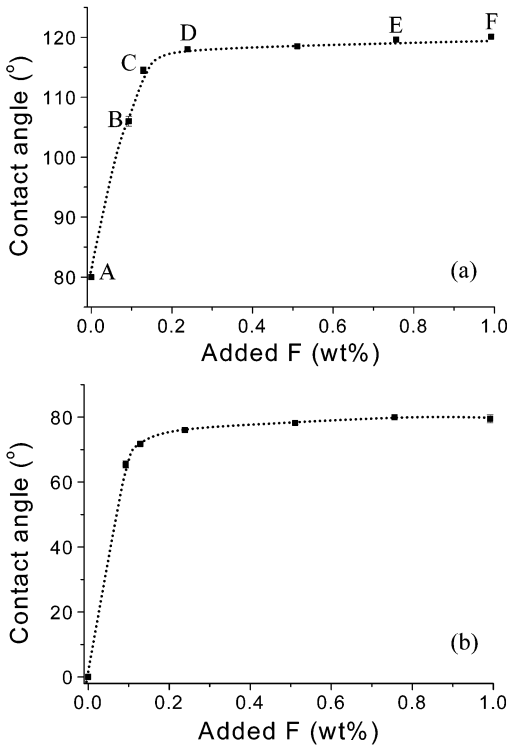

Figure 5. Advancing contact angles of water (a) and static contact angles of hexadecane (b) on polymer films, from SLO and F6-N3300 cured at 80 °C, as a function of the added fluorine content in the films.

F6-HDI on the films indicates that the driving force for the surface enrichment of fluorine is a bit stronger for F8-HDI than for F6-HDI, due to the longer perfluoroalkyl chain in the former.

For the films from a mixture of F6-N3300, N3300, and SLO, the water advancing contact angle increased from 80° to 120° as the fluorine concentration increased from 0 to 1.0 wt %, as shown Figure 5a. The high contact angles indicate that the film surface is dominantly enriched in the fluorinated species. A plateau was reached at a fluorine concentration of about 0.4 wt %. A similar trend given in Figure 5b was observed for the static contact angles of hexadecane on the films. Without fluorine present in the films, hexadecane could spread over the surface; once there was a small amount of fluorine, the contact angle jumped to 65° and then leveled off at around 80°. By using the geometric mean method,[35] the lowest surface energy for this series of films was calculated to be around 10 mN/m. The films on the basis of F8-N3300 and SLO gave similar results. In comparison with the films based on partially fluorinated oligoesters and normal N3300 in which the lowest surface energy was around 25 mN/m,[30] the surface energy for the films in the current study is significantly lower. This clearly suggests that, for the films prepared from partially fluorinated isocyanates and liquid oligoesters, there is even more pronounced surface segregation of fluorinated species.

The low surface energy films were either rinsed by water or rubbed by acetone; the difference of the water advancing contact angles was less than 2°, implying that the fluorinated tail was chemically bonded to the cross-linked films and the film surface was quite stable.

It is a bit of surprise to notice that films from F6-N3300 showed more pronounced surface segregation of fluorinated species than those from F6-HDI and, even, F8-HDI. F6-HDI and F8-HDI are smaller molecules than F6-N3300, and they are supposed to diffuse faster than F6-N3300 in the reactive mixture. However, as clearly shown earlier by FTIR studies (Figure 3), HDI reacts much more rapidly with SLO than N3300, so the viscosity of the reaction mixture of HDI and SLO may become very high in a very short period of time, which may limit the diffusion of fluorinated species to migrate toward the air/film interface. In contrast, although the starting viscosity of N3300/SLO was higher than that of HDI/SLO, the increase of viscosity of the former would be much slower than the latter; as a consequence, the slower cross-linking may allow more time for fluorinated species to diffuse to the air/film interface, resulting in a more significant surface enrichment of fluorine. The films on the basis of F6-N3300/SLO were chosen for other surface characterizations.

Recently, Thomas et al.[22] reported the surface properties of films from reactive mixtures of methacrylate copolymers and fluorinated N3300 (similar to the one in the current study), but the reported contact angles for both water (~86°) and hexadecane (40°) were significantly lower than those in the current study. When surface active perfluoroalkylethyl methacrylate copolymers were combined with the fluorinated N3300, higher contact angles (water, 110°; hexadecane, 63°) were observed; the higher contact angles were claimed to be ascribed to the more surface active perfluorinated copolymer which was synthesized by the so-called "single shot addition" copolymerization.[21] The higher contact angles might be due to the existence of a small amount of fluorinated homopolymers formed during the "single shot addition" copolymerization. Even in this case, the contact angles are lower than those in the current study. Our results unambiguously indicate that the partially fluorinated isocyanates are very surface

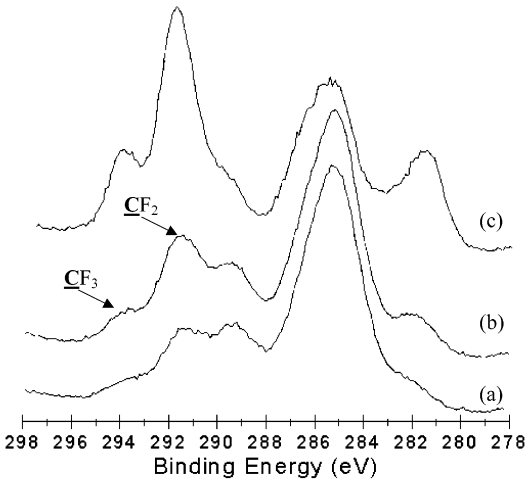

Figure 6. XPS C_{1s} spectra for a film from SLO and F6-N3300 cured at 80 °C with a fluorine content of 1 wt % (sample F in Figure 5). Takeoff angles: (a) 75°, (b) 45°, and (c) 15°.

active. We believe that this is likely due to the lower viscosity for the reactive mixtures in the current study since the mixtures are composed of partially fluorinated isocyanates and solventless liquid oligoesters of low viscosities. The lower viscosity of the reactive mixtures would facilitate the diffusion of fluorinated species toward the air/film interface, leading to a strong surface enrichment of fluorinated species at the surface. Since there was basically no organic solvent involved, the low surface energy polymeric films were obtained in an environmentally friendly way.

Chemical Compositions at the Film Surfaces. The surface enrichment of the fluorinated species in the films was also investigated by XPS. In XPS experiments, the sample of interest was irradiated with Mg Kα X-rays as the kinetic energy of the emitted photoelectron was recorded. The analysis depth, d, is controlled by the mean free path[36] of the ejected photoelectron through the following simplified equation[37]

$$d = 3\lambda \sin \theta$$

where λ is the inelastic mean free path of the electron and θ is the takeoff angle. A nondestructive depth profile analysis of up to 7.3 nm (for carbon)[36] can be obtained by changing the takeoff angle. In our experiments, the takeoff angles of 15°, 45°, and 75° correspond to the detection depths for carbon of approximately 1.9, 5.2, and 7.1 nm, respectively.

The C_{1s} regions of the XPS spectra at different takeoff angles for a film with about 1 wt % of fluorine (sample F in Figure 5), cured at 80 °C from a mixture of SLO and F6-N3300, are shown in Figure 6. In the C_{1s} region of these spectra, discrete peaks can be assigned to different functional groups, including (in the order of increasing binding energy; curve-fitting data not shown) C−H, C−O/C−N, C═O, CF_2, and CF_3,[21,30] among which CF_2 and CF_3 are marked with arrows in the figure. Obviously, when the probe depth gets shallower (smaller takeoff angles), the peak intensities due to CF_2 and CF_3 become greater. There is a gradient distribution of the fluorinate species from the surface down to the bulk, similar to what was reported by Schmidt et al. on nonstick surfaces made from reactive perfluoroalkyl polymeric surfactants.[4,17]

As the fluorine content in the film increased from 0 to 1 wt %, the peaks corresponding to CF_2 and CF_3 became more and more obvious. In Figure 7 is given the F/C atomic ratio as a function of the added fluorine content in the films. The overall F/C atomic ratio in the films was lower than 0.01, but in the first about 7 nm of the films much more fluorine-containing species segregated. For example, when the added F/C ratio was only 0.0027, the surface F/C atomic ratio was 1.1, 0.71, and 0.46 at takeoff angles of 15°, 45°, and 75°, respectively. In this series of samples, the surface excess of fluorine at a depth of about 5.2 nm ranged from 60- to 600-fold above the added levels, and the surface excess in the first 7.1 nm depth was 50−390-fold above the added levels. This surface enrichment of fluorine is much more significant than that in the films on the basis of fluorinated oligoesters and normal N3300, where an enrichment factor of 30−80 in the first about 5 nm was observed.[30] This is primarily due to the more favorable diffusion of the fluorinated polyisocyanate toward the air/film interface, due to its smaller molecular size, than that of the fluorinated oligoester.

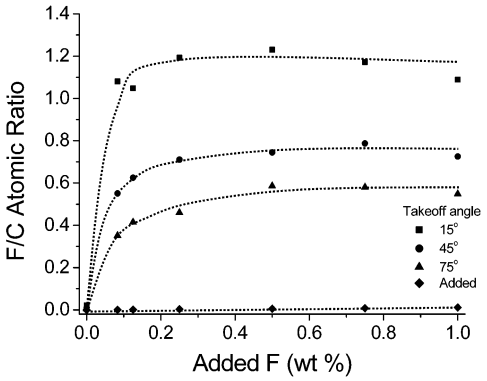

Figure 7. Surface F/C atomic ratio as a function of the added fluorine content in the films from SLO and F6-N3300 cured at 80 °C.

Table 2. Surface Energies (mN/m) of Isocyanates before and after Partial Fluorination

liquid	C_nF_{2n+1}/NCO	surface energy
HDI		40.2 ± 0.1
C_6F_{13}−$(CH_2)_2$−OH (F6-OH)		16.6 ± 0.2
F6-HDI-I	1/199	35.8 ± 0.1
F6-HDI-II	1/99	32.8 ± 0.1
F8-HDI	1/99	26.5 ± 0.1
theoretical value by group contribution theory (Parachor)		
HDI		39.3 ± 7.0[a]
F6-OH		16.4 ± 3.0[a]
F6-HDI-Parachor	1/1	25.7 ± 7.0[a]
F8-HDI-Parachor	1/1	24.2 ± 7.0[a]

[a] The error was provided by ChemSketch.

Figure 7 also clearly indicates that the surface F/C ratio becomes almost unchanged at the fluorine content of about 0.5 wt %, in agreement with the contact angle data depicted in Figure 5. Thus, a surface strongly enriched in fluorine can be created with the addition of fluorinated species containing only 1 wt % of fluorine in the mixture.

Driving Force for Surface Segregation of Fluorinated Species. To illustrate the driving force for the surface segregation of fluorinated species, surface energies of some liquids were measured by the Wilhelmy plate method, as given in Table 2. Since the viscosity for N3300 and fluorinated N3300 is quite high and it is very difficult to reach equilibrium during measurements, their surface energies are not measured by the Wilhelmy plate method. It is clearly shown that the

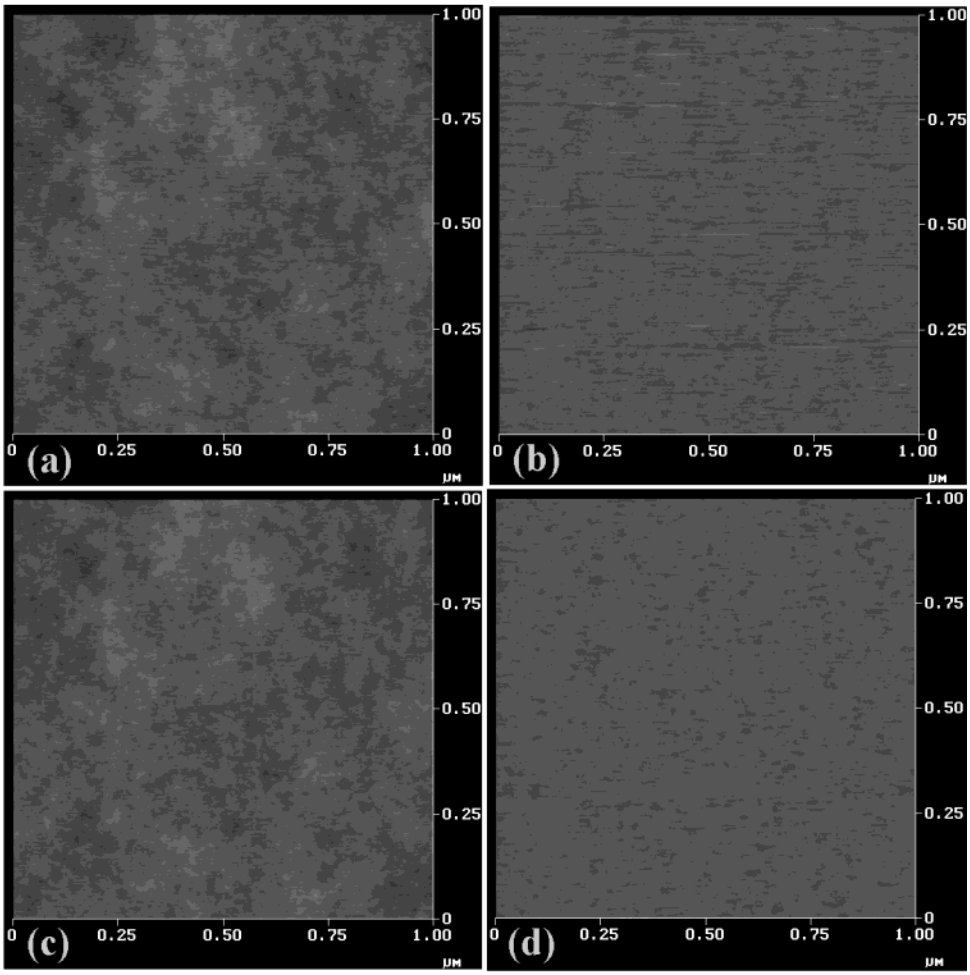

Figure 8. AFM height (left, *z*-scale: 20 nm) and phase (right, *z*-scale: 20°) images for films (sample A in Figure 5) containing no fluorine on the basis of SLO and N3300; tapping force (starting amplitude set point: 0.59 V): amplitude, top 0.39 V, and bottom 0.20 V.

fluorinated HDI (F6-HDI-I) had a lower surface energy (35.8 mN/m) than HDI (40.2 mN/m) even when only 1 out of 200 NCO groups was substituted by $-C_6F_{13}$. The fluorinated HDI with a higher concentration of fluorine (F6-HDI-II) had an even lower surface energy, 32.8 mN/m. The fluorinated HDI (F8-HDI) with a longer fluorinated tail gave a much lower surface energy (26.5 mN/m). On the other hand, the surface energy of the liquid oligoester was determined to be around 42 mN/m. The large difference in the surface energy between the fluorinated species and nonfluorinated components contributes to the driving force of surface segregation of the fluorinated species.

Also shown in Table 2 are the theoretical surface energies estimated from the so-called group contribution theory (Parachor).[38,39] First of all, there is a good agreement between the theoretical and experimental values for HDI and F6-OH, implying the validity of the group contribution theory. The surface energies for perfluoroalkyl monosubstituted HDIs (F6-HDI-Parachor and F8-HDI-Parachor) were estimated to be 25.7 and 24.2 mN/m, respectively. Comparing these two values with the surface energies of HDI and the liquid oligoester (both around 40 mN/m), the "real" difference in surface energy between the fluorinated species and nonfluorinated components would be as large as 15−16 mN/m, which ensures a strong driving force for the fluorinated species to migrate toward the air/film interface.

Topological Investigations on Fluorinated Surfaces. It is known that, besides the surface chemical composition, the surface roughness also plays a very important role in determining the wettability of a film.[40] Tapping mode AFM with simultaneous topographical and phase detection has been successfully used to demonstrate both the nanoscale surface roughness[4,17] and the nanoscale surface chemical resolution via mechanical differences of the different domains.[41−43] In the phase data under light or moderate tapping force, the lighter areas are usually ascribed to stiffer materials, whereas the darker areas correspond to soft materials.[43]

AFM height and phase images for the fluorine-free films on the basis of SLO and N3300 under light (set point amplitude adjusted to 75−90% of the free air amplitude) and moderate force (set point amplitude adjusted to 40−70% of the free air amplitude)[43] are shown in Figure 8. In the scan box of 1 μm × 1 μm, the root-mean-square (rms) roughness is around 0.3 nm for both height images (Figure 8a,c). The wettability behavior of films would not be affected by such a small roughness variation. The phase images are essentially featureless under two different tapping forces (the tapping force for the bottom image (d) was about 40% higher than the upper image (b)). It indicates that, as expected, the chemical composition is quite uniformly distributed along the surface.

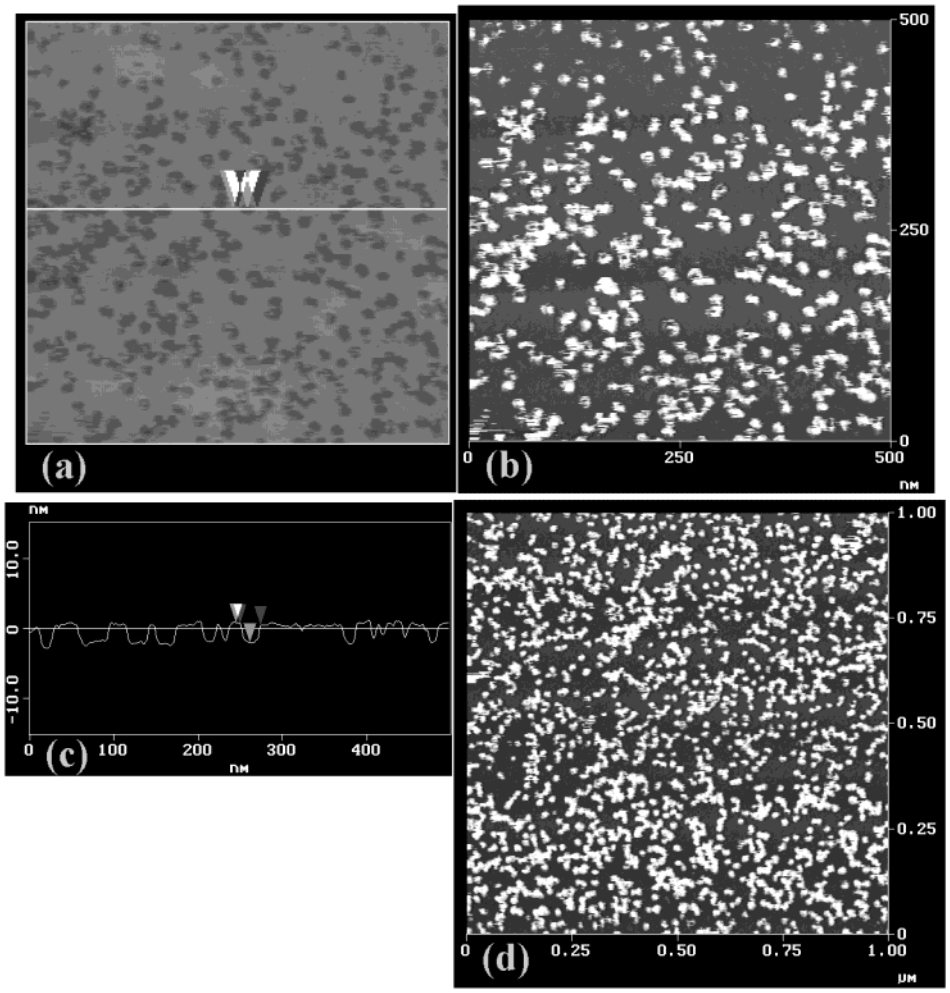

Figure 9. AFM height [(a) *z*-scale: 20 nm] and phase [(b) and (d), *z*-scale: 100°] images for films (sample E in Figure 5) containing 0.75 wt % fluorine on the basis of SLO and F6-N3300, under light-force tapping mode. Shown in (c) is the topological profile on the basis of (a).

For the films containing fluorine, on the other hand, totally different topographical and phase images were obtained. In Figure 9 both height and phase images for a film containing about 0.75 wt % of fluorine (sample E in Figure 5) are given under light tapping force (sample F in Figure 5 containing about 1 wt % of fluorine showed similar images). Some domain structures can be easily identified in both height and phase data. It is interesting to note that the domains appear to be "low spots" in the topographic image. The "low spots" are typically 2−3 nm below the surface and typically with a lateral diameter of 15−25 nm, as shown in Figure 9c. These "low spots" are believed to correspond to the more hydrophobic materials, i.e., fluorocarbon-rich domains in this case; this phenomenon is consistent with some early findings on a fluorinated alkyd resin.[43] On the other hand, these "low spots" appeared to be the "light" domains in the phase images (Figure 9b,d). When the scan box size was increased from 0.5 μm × 0.5 μm (b) to 1 μm × 1 μm (d), the number of domains apparently quadrupled. In accordance to some previous studies,[43,44] we believe that these "light" domains are rich in the fluorinated species. (They are stiffer than non-fluorinated species in this study.) The continuous dark area is, therefore, fluorine-poor.

When the tapping force increases, the phase contrast may be enhanced. Shown in Figure 10 are changes in height and phase images for the same sample as in Figure 9 under the influence of different tapping forces. When the tapping force increased from "light" force (Figure 10a) to "light moderate" force (Figure 10c) and "heavy moderate" force (Figure 10e), topographical feature became less pronounced. This is probably due to the fact that, under stronger tapping forces, the elastic response from different materials (fluorine-rich and fluorine-poor) may become indistinguishable to the tip. On the other hand, the changes in phase images are more intriguing. The upper right image (Figure 10b) under light tapping force was similar to the one shown in Figure 9b; light and dark areas were clearly visible. When the tapping force increased to "light moderate", the phase contrast became less obvious (Figure 10d). Even the dark area turned much lighter, which may imply, to some extent, that the dark area in Figure 10b also contains some fluorinated species although it is poor in fluorine. Nevertheless, the domains can still be distinguished in Figure 10d. When the tapping force further increased to "heavy moderate", it became much more difficult to distinguish the domains in Figure 10f. Almost the whole area became light, and only a small fraction of area was dark. Here we see how the tapping force can alter the phase contrast. One has to be cautious when analyzing a phase image.

We changed the "heavy moderate" force back to "light" force for the same scanning box. Interestingly, both topographic and phase images were essentially the same

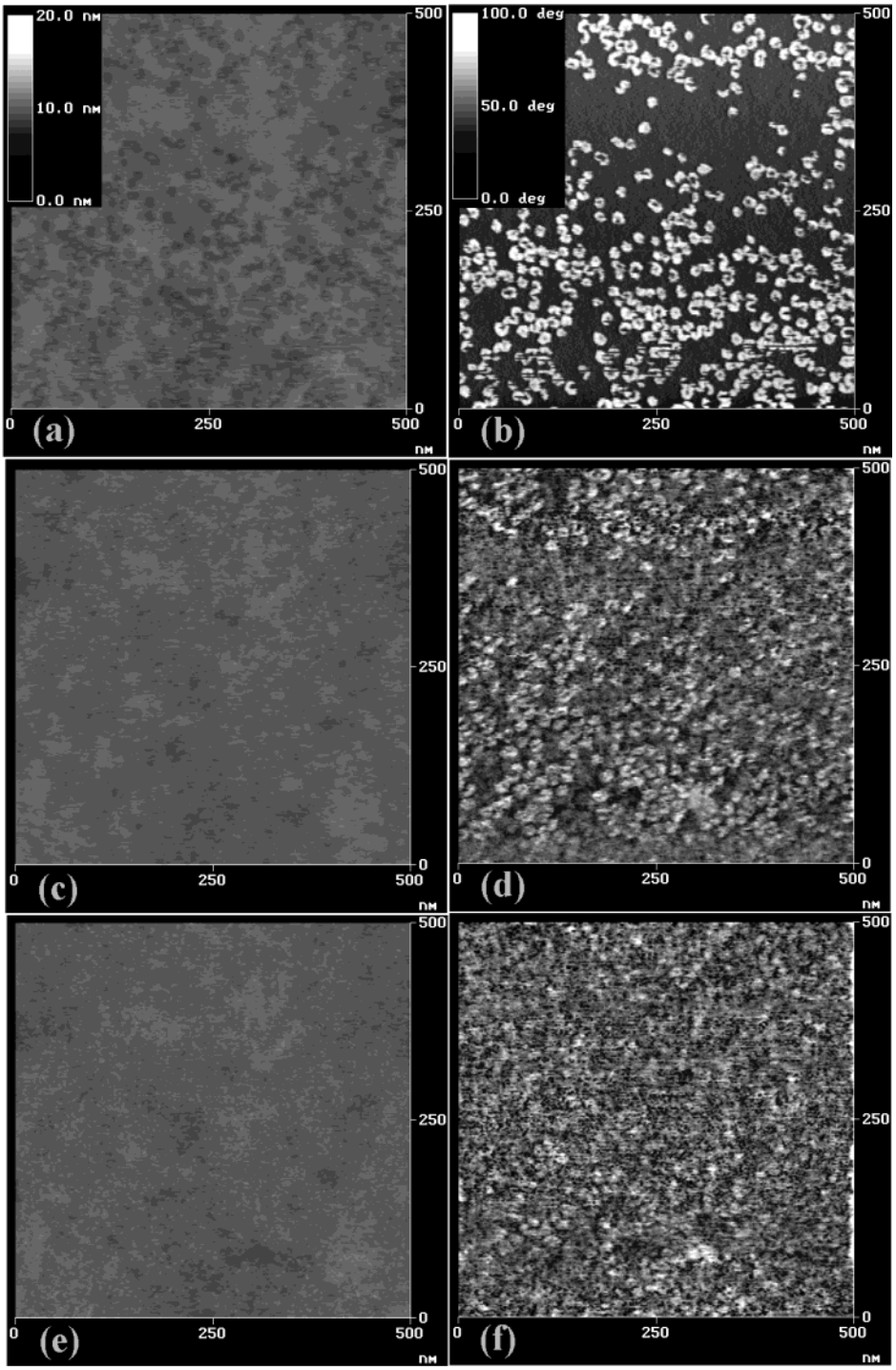

Figure 10. AFM height (left, *z*-scale: 20 nm) and phase (right, *z*-scale: 100°) images for films (sample E in Figure 5) containing 0.75 wt % fluorine on the basis of SLO and F6-N3300, under different tapping forces (starting amplitude set point: 0.48 V): amplitude, top 0.44 V, middle 0.35 V, and bottom 0.24 V.

with Figure 10a,b. Therefore, the tapping force did not damage the film surface, and more importantly, the reversibility of the images suggests that the phase contrast we observed is indeed not due to the different AFM operation conditions, but due to the inherent surface chemical heterogeneity.

We also collected the phase images under light tapping forces for the films containing less amounts of fluorine, as shown in Figure 11. Images (a), (b), (c), and (d) correspond to the films (B), (C), (D), and (E) in Figure 5, respectively. When the film contained only 0.09 wt % of fluorine, only tiny light domains in the size of less than 2−3 nm were visible (Figure 11a). When the fluorine concentration increased to 0.13 wt %, the domain size did not change much (Figure 11b), but the number of light domains became much larger. The further increase of fluorine concentration led to the formation of much larger domains in Figure 11c. At this concentration, we see the starting of the plateau for both the contact angles (Figure 5) and the fluorine contents at the surface (Figure 7). Round domains could be observed when the fluorine concentration was even higher (Figure 11d), which is the same with Figure 9b. It is interesting to note that, although the surface

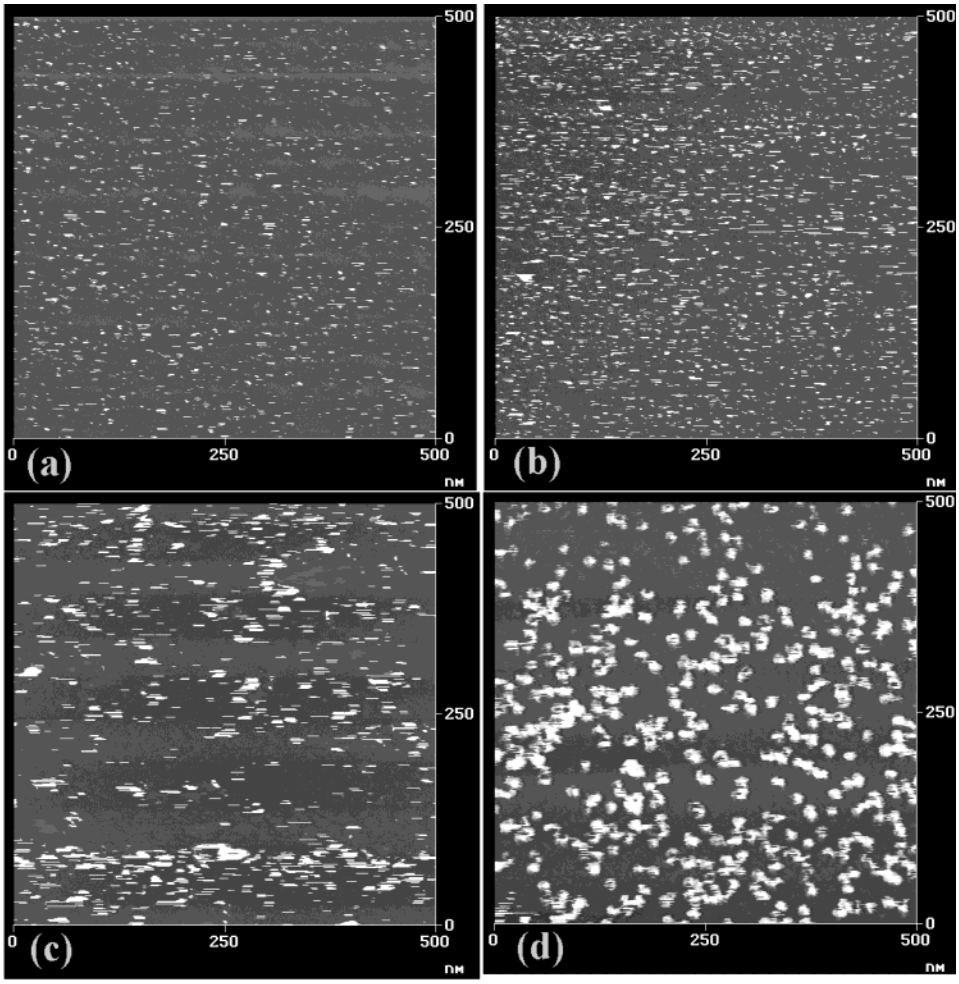

Figure 11. AFM phase images (*z*-scale: 100°) under light tapping forces for polymeric films from SLO and F6-N3300 cured at 80 °C. The added fluorine concentrations (wt %) were (a) 0.09, (b) 0.13, (c) 0.24, and (d) 0.75.

topologies are not the same for the films containing different amounts of fluorine (from 0.25 to 1.0 wt %), the contact angle data and fluorine contents at the surface for these films appear to be similar. It has been shown that, for a surface fully covered by $-CF_3$ groups, high contact angles (water, 120°; hexadecane, 80°) can be obtained.[45] From this study, it appears, however, that high contact angles and low wettability can be achieved by *nanoscale* phase-separated fluorinated surfaces. It is, therefore, possible to use very small amounts of fluorinated species to obtain extremely low wettability.

The formation of fluorine-enriched domains may be a consequence of the formation of cross-linked networks. If there were no cross-linking involved, the fluorinated species would first segregate at the surface. Because of the hydrophobic interaction among fluorinated tails, some droplets may form and eventually, probably, end up with a thin layer at the top of the film when the fluorine concentration is high enough, instead of the formation of the domain structure as shown above. But when cross-linking takes place during the film formation, the system becomes immobilized in a period of time, and the fluorine-rich aggregates would be frozen, leading to the formation of the domains.

As mentioned in the Introduction, we prepared some low surface energy films from partially fluorinated liquid oligoesters and normal N3300.[30] By introducing up to 1.5 wt % of fluorine in the films, surface energies could be reduced to around 25 mN/m. Topographic and phase images were also collected for a film containing 1.43 wt %, which is the film F-4 in the previous paper.[30] Both height and phase images (data not shown, but essentially the same with Figure 8) are almost featureless under the light tapping force. When the tapping force increased from "light" to "heavy moderate", the images remained essentially the same. This clearly suggests that the distribution of fluorinated species is quite homogeneous even at the nanometer scale at the surface for this film; at least it is not discernible by the AFM technique under current conditions. The lower fluorine concentration at the surface, in comparison with the films in the current study, was also evidenced by XPS.[30] The less pronounced surface segregation of fluorinated species is likely due to the less favorable diffusion of the fluorinated oligoester molecules, partly because of their larger molecular sizes and partly because of their stronger H-bonding interactions with non-fluorinated hydroxyl-containing oligoesters. Currently efforts are being taken in our laboratory to gain more understanding on the competition behaviors between the diffusion of fluorinated species and the formation of cross-linked networks.

Conclusions

It has been demonstrated in this paper that polymeric films with surface energies as low as 10 mN/m can be readily prepared by thermally curing a mixture of hydroxyl-end-capped liquid oligoesters and partially

fluorinated polyisocyanates. It has been shown from the contact angle and XPS investigations that a low fluorine level (<1.0 wt %) is sufficient in producing very low surface energies. The favorable diffusion of small fluorinated molecules contributed to their strong surface segregation. The fluorine levels in the first a few nanometers of the film are dozens to hundreds of times greater than in the bulk. When there was 0.5−1.0 wt % of fluorine in the system, some fluorine-enriched domains in the size of 15−25 nm were formed at the film surface, as a consequence of the competition between the diffusion of fluorinated species and the formation of cross-linked network. These fluorinated nanodomains are believed to lead to the low wettability of the films. Such low surface energy films may provide many interesting properties, such as low coefficients of friction, excellent water/oil repellency, possibly self-cleanability, and so on.

Acknowledgment. We appreciate the beneficial discussions with Prof. G. de With. This study was financially supported by the Dutch Organization for Scientific Research (CW-NWO) in the Priority Program for Materials Research (PPM), the Graduate School MTC/MATTeR at Eindhoven University of Technology, and INCO-Copernicus Grant IC15-CT980822 from European Union.

References and Notes

(1) Grainger, D. W., Castner, D. G., Eds.; *Fluorinated Surfaces, Coatings and Films*; ACS Symposium Series 787; American Chemical Society: Washington, DC, 2001.
(2) Hougham, G., Cassidy, P. E., Johns, K., Davidson, T., Eds.; *Fluoropolymers 1 & 2*; Kluwer Academic/Plenum Publishers: New York, 1999.
(3) Scheirs, J., Ed.; *Modern Fluoropolymers*; Wiley: New York, 1997.
(4) Schmidt, D. L.; Coburn, C. E.; DeKoven, B. M.; Potter, G. E.; Meyers, G. F.; Fischer, D. A. *Nature (London)* **1994**, *368*, 39.
(5) Anton, D. *Adv. Mater.* **1998**, *10*, 1197.
(6) PFPEs are commercialized by Ausimont under the trademark of Fluorobase.
(7) For example: (a) Bongiovanni, R.; Malucelli, G.; Lombardi, V.; Priola, A.; Siracusa, V.; Tonelli, C.; Di Meo, A. *Polymer* **2001**, *42*, 2299. (b) Casazza, E.; Mariani, A.; Ricco, L.; Russo, S. *Polymer* **2002**, *43*, 1207. (c) Toney, M. F.; Mate, C. M.; Leach, K. A. *Appl. Phys. Lett.* **2000**, *77*, 3296.
(8) FEVE copolymers are commercialized by Asahi Glass, Co., under the trademark of LUMIFLON.
(9) For example: (a) Lousenberg, R. D.; Shoichet, M. S. *J. Polym. Sci., Part A: Polym. Chem.* **2000**, *38*, 1344. (b) Yuan, Y.; Shoichet, M. S. *Macromolecules* **1999**, *32*, 2669.
(10) Yoon, S. C.; Ratner, B. D. *Macromolecules* **1986**, *19*, 1068; **1988**, *21*, 2392, 2401.
(11) Yoon, S. C.; Ratner, B. D.; Ivan, B.; Kennedy, J. P. *Macromolecules* **1994**, *27*, 1548.
(12) Höpken, J.; Möller, M. *Macromolecules* **1992**, *25*, 1461.
(13) Champan, T. M.; Marra, K. G. *Macromolecules* **1995**, *28*, 2081.
(14) Kassis, C. M.; Steehler, J. K.; Betts, D. E.; Guan, Z. B.; Romack, T. J.; DeSimone, J. M.; Linton, R. W. *Macromolecules* **1996**, *29*, 3247.
(15) Sun, F.; Castner, D. G.; Mao, G.; Wang, M.; McKeown, P.; Grainger, D. W. *J. Am. Chem. Soc.* **1996**, *118*, 1856.
(16) Affrossman, S.; Bertrand, P.; Hartshorne, M.; Kiff, T.; Leonard, D.; Pethrick, R. A.; Richards, R. W. *Macromolecules* **1996**, *29*, 5432.
(17) Schmidt, D. L.; DeKoven, B. M.; Coburn, C. E.; Potter, G. E.; Meyers, G. F.; Fischer, D. A. *Langmuir* **1996**, *12*, 518.
(18) Iyengar, D. R.; Perutz, S. M.; Dai, C.; Ober, C. K.; Kramer, E. J. *Macromolecules* **1996**, *29*, 1229.
(19) Wang, J. G.; Mao, G. P.; Ober, C. K.; Kramer, E. J. *Macromolecules* **1997**, *30*, 1906.
(20) Xiang, M.; Li, X.; Ober, C. K.; Char, K.; Genzer, J.; Sivaniah, E.; Kramer, E. J.; Fischer, D. A. *Macromolecules* **2000**, *33*, 6106.
(21) Thomas, R. R.; Anton, D. R.; Graham, W. F.; Darmon, M. J.; Sauer, B. B.; Stika, K. M.; Swartzfager, D. G. *Macromolecules* **1997**, *30*, 2883.
(22) Thomas, R. R.; Anton, D. R.; Graham, W. F.; Darmon, M. J.; Stika, K. M. *Macromolecules* **1998**, *31*, 4595.
(23) Thomas, R. R.; Glaspey, D. F.; DuBois, D. C.; Kirchner, J. R.; Anton, D. R.; Lloyd, K. G.; Stika, K. M. *Langmuir* **2000**, *16*, 6898.
(24) Mason, R.; Jalbert, C. A.; O'Rourke Muisener, P. A. V.; Koberstein, J. T.; Elman, J. F.; Long, T. E.; Gunesin, B. Z. *Adv. Colloid Interface Sci.* **2001**, *94*, 1.
(25) Winter, R.; Nixon, P. G.; Terjeson, R. J.; Mohtasham, J.; Holcomb, N. R.; Grainger, D. W.; Graham, D.; Castner, D. G.; Gard, G. L. *J. Fluorine Chem.* **2002**, *115*, 107.
(26) van de Grampel, R. D.; Ming, W.; Laven, J.; van der Linde, R.; Leermakers, F. A. M. *Macromolecules* **2002**, *35*, 5670.
(27) Funke, W. *Prog. Org. Coat.* **1973/74**, *2*, 289; *J. Oil Col. Chem. Assoc.* **1976**, *59*, 398.
(28) Verkholantsev, V. V. *Prog. Org. Coat.* **1985**, *13*, 71; *J. Coat. Technol.* **1992**, *64* (809), 51; *Prog. Org. Coat.* **1995**, *26*, 31.
(29) (a) Carr, C.; Wallstom, E. *Prog. Org. Coat.* **1996**, *28*, 161. (b) Benjamin, S.; Carr, C.; Walbridge, D. J. *Prog. Org. Coat.* **1996**, *28*, 197. (c) Vink, P.; Bots, T. L. *Prog. Org. Coat.* **1996**, *28*, 173.
(30) Ming, W.; Laven, J.; van der Linde, R. *Macromolecules* **2000**, *33*, 6886.
(31) Ming, W.; van Ravenstein, L.; van de Grampel, R.; van Gennip, W.; Krupers, M.; Niemantsverdriet, H.; van der Linde, R. *Polym. Bull. (Berlin)* **2001**, *47*, 321.
(32) Ming, W.; Lou, X.; van de Grampel, R. D.; van Dongen, J. L. J.; van der Linde, R. *Macromolecules* **2001**, *34*, 2389.
(33) Ming, W.; Melis, F.; van de Grampel, R. D.; van der Linde, R.; et al. Submitted to *Proceedings of 2002 Athens Conference on Coatings Science & Technology*, pp 189−197.
(34) Johnson, R. E., Jr.; Dettre, R. H. In *Wettability*; Berg, J. C., Ed.; Marcel Dekker: New York, 1993; Chapter 1.
(35) (a) Owens, D. K.; Wendt, R. C. *J. Appl. Polym. Sci.* **1969**, *13*, 1741. (b) Kaelble, D. H. *J. Adhes.* **1970**, *2*, 50.
(36) Briggs, D. *Surface Analysis of Polymers by XPS and Static SIMS*; Cambridge University Press: Cambridge, 1998; Chapter 2.
(37) Kissa, E. *Fluorinated Surfactants: Synthesis, Properties, Applications*; Marcel Dekker: New York, 1993; p 386.
(38) Van Krevelen, D. W. *Properties of Polymers: Their Estimation and Correlation with Chemical Structure*, 3rd ed.; Elsevier: Amsterdam, 1997; Chapter 8.
(39) The calculations were done by using ChemSketch, version 3.50, developed by Advanced Chemistry Development Inc., Toronto, Canada.
(40) Wu, S. *Polymer Interface and Adhesion*; Marcel Dekker: New York, 1982; Chapter 1.
(41) Magonov, S. N.; Elings, V.; Whangbo, M.-H. *Surf. Sci.* **1997**, *375*, L385.
(42) McLean, R. S.; Sauer, B. B. *Macromolecules* **1997**, *30*, 8314.
(43) Sauer, B. B.; McLean, R. S.; Thomas, R. R. *Langmuir* **1998**, *14*, 3045.
(44) Ebbens, S. J.; Badyal, J. P. S. *Langmuir* **2001**, *17*, 4050.
(45) For instance: Schönherr, H.; Ringsdorf, H. *Langmuir* **1996**, *12*, 3891.

MA020650I